

To appear in *Philosophical Magazine*, 1996.

# Low-Energy Excitations in an Incipient Antiferromagnet

*D. W. Hess*

Complex Systems Theory Branch  
 Naval Research Laboratory  
 Washington, D.C. 20375-5345

*J. J. Deisz and J. W. Serene*

Department of Physics  
 Georgetown University  
 Washington, D.C. 20057-0995

**Abstract:** We present fully self-consistent calculations in the fluctuation exchange approximation for the half-filled Hubbard model in 2D. A non-fermi liquid state evolves with decreasing temperature in this self-consistent model of coupled spin fluctuations and quasiparticles. The mean field phase transition to long-range antiferromagnetic order is suppressed and we find no evidence of a phase transition to long-range magnetic order. We show that the real part of the self-energy at zero energy shows a positive slope and the imaginary part of the self-energy shows a local minimum. The scale of this structure is set by the zero temperature gap in mean field theory. The growth of spin fluctuations is reflected in the evolution of sharply peaked structure in the spin fluctuation propagator around zero energy and  $\mathbf{Q} = (\pi, \pi)$ . We present calculations for the Hubbard model in 1D in a two-particle self-consistent parquet approximation. A second moment sum rule suggests that vertex corrections to the self-energy are responsible for the greater accuracy of the parquet approximation as compared to other self-consistent perturbation theories.

## §1 *Introduction and Physical Picture*

The role of spin fluctuations in the physics of a many-body Fermi system seems a particularly appropriate topic for a festschrift in honor of David Pines. In liquid  $^3\text{He}$ , ferromagnetic spin fluctuations play a central role in the normal and superfluid states. The exchange of spin fluctuations contributes a non-analytic correction to the quasiparticle energy that is reflected in finite-temperature corrections to the transport properties and specific heat predicted by Landau Fermi liquid theory (Baym and Pethick, 1991). Similar corrections were also found for metallic systems near a ferromagnetic instability

(Berk and Schrieffer 1966, Doniach and Englesberg 1966). In both heavy fermion materials and the high-temperature superconductors, the close proximity of antiferromagnetic instabilities and the observation of unusual and possibly unconventional superconductivity has aroused interest in the role of antiferromagnetic spin fluctuations, both as an explanation of the unusual normal state properties and as a pairing mechanism.

The normal-state properties of the high-temperature superconductors have inspired speculations that interplay among correlations, low dimensionality and the tendency to magnetic order could give rise to low-energy excitations that are not adequately described by the Landau theory of a Fermi liquid. Varying degrees of departure from Landau theory have been proposed (for recent reviews, see Kampf (1994) and Dagotto (1994)), ranging from the ‘soft singularities’ of phenomenological marginal Fermi liquids and nearly antiferromagnetic Fermi liquids to more dramatic conjectures of separation of charge and spin excitations such as Luttinger liquids (Anderson, 1990). All the proposed departures from a Fermi liquid description of low energy excitations ultimately rest on subtle features of interactions between renormalized quasiparticles. Thus a self-consistent approach seems necessary for a complete and satisfactory theory. The observation of an antiferromagnetically ordered state in the parent compounds of the high temperature superconductors suggests the possibility that the renormalization of quasiparticle excitations by the exchange of spin fluctuations may account for the unusual properties of these materials. Here we describe results for a self-consistent model aimed at elucidating the physics of coupled spin fluctuations and quasiparticle excitations.

The 2D copper-oxide layer structure of the cuprate high temperature superconductors has inspired great interest in the single-band Hubbard Hamiltonian in 2D as a model for the high temperature superconductors (Anderson, 1987). Numerical evidence from quantum Monte Carlo calculations strongly indicates that the ground state of the half-filled Hubbard model in 2D possess long-range antiferromagnetic order (Hirsch and Tang, 1989; White, Scalapino, Sugar, Loh, Gubernatis, and Scalettar, 1989); at finite temperature, the possibility of long-range magnetic order is precluded by the Mermin-Wagner theorem. In this paper we consider the 2D Hubbard model at half-filling, where spin fluctuations are expected to play a pivotal role as the system of coupled quasiparticles and (incoherent) spin fluctuations self-consistently evolves with decreasing temperature toward the ordered state at zero temperature. For small  $U$ , mean field theory predicts a phase transition to an antiferromagnetically ordered state at a non-zero temperature.

In a previous work (Deisz, Hess and Serene, 1995) we showed that the self-consistent inclusion of fluctuations at the level of the fluctuation exchange approximation (FEA) strongly suppresses the mean field phase transition; we have not observed a magnetic phase transition down to the lowest temperatures for which we have calculations. At sufficiently low temperature, the coupling of growing spin fluctuations to quasiparticle excitations leads to the evolution of a non-Fermi liquid state, clearly signaled by anomalous features in the self-energy for  $\varepsilon \sim 0$ : a positive slope in the real part and a local minimum in the imaginary part. Spectral weight is rapidly pushed away from the Fermi surface with decreasing temperature leading to the formation of a weak pseudogap in the single-particle density of states. We presented a simple analytical model which showed that these features, along with developing shadow structure in single-particle spectral functions, are a consequence of evolving spin fluctuations and their self-consistent effect on the structure of evolving quasiparticles.

This paper extends our previous results providing further details of the evolution of

the non-Fermi liquid state with decreasing temperature. We observe that the structure that develops in the self-energy at low energy occurs on the scale of the zero temperature gap in mean field theory. The formation of the non-Fermi liquid state is accompanied by the evolution of a sharply peaked structure in the  $T$ -matrix; the temperature and energy dependence of this structure suggests the existence of a strongly temperature dependent characteristic energy scale not unlike that proposed in the phenomenologically motivated NAFL (Pines, 1990; Millis, Monein and Pines, 1990). To make this discussion self contained, we briefly summarize the FEA in the next section. In §3 we present a short summary of our numerical methods; it will be convenient there to summarize some formally exact results that suggest that FEA is a better approximation than including only the sum of the particle-hole bubble diagrams (the shielded potential approximation). In §4 we describe the non-Fermi liquid solution that evolves at low temperature. Finally in §5, we present results for the 1D Hubbard model at half filling in a fully self-consistent parquet approximation. This approximation includes interactions between fluctuations in the calculation of the self-energy and is self-consistent at the level of the two-particle propagator.

## §2 The Fluctuation Exchange Approximation for the Hubbard Model

In the propagator renormalized perturbation theory of Luttinger and Ward (Luttinger and Ward, 1960) the grand thermodynamic potential  $\Omega$  is constructed as an independent functional of the fully renormalized single particle propagator  $G$  and the self-energy  $\Sigma$ , and is stationary with respect to independent variations of  $G$  and  $\Sigma$ . Dyson's equation follows from

$$\frac{\delta\Omega[G, \Sigma]}{\delta\Sigma} = 0, \quad (1)$$

and the representation of the self-energy as a sum of ‘skeleton’ graphs evaluated with the fully renormalized propagator and bare two-particle vertex is obtained from

$$\frac{\delta\Omega[G, \Sigma]}{\delta G} = 0. \quad (2)$$

The self-consistent solution of Eq. (1) and Eq. (2) yields the exact Green's function. Explicit summation of the infinite set of ‘skeleton’ graphs for the self-energy required for the exact solution is generally not possible and approximations are generated by selecting a class or classes of vacuum graphs for the grand potential. The FEA is one such approximation; it includes the exchange of density fluctuations, spin-density fluctuations and singlet-pair fluctuations.

It is convenient to discuss the FEA by alternating between position and (imaginary) time, and momentum and (imaginary) frequency representations. The FEA for the electron self-energy of the paramagnetic state is given by

$$\Sigma(\mathbf{r}, \tau) = U^2 [\chi_{ph}(\mathbf{r}, \tau) + T_{\rho\rho}(\mathbf{r}, \tau) + T_{sf}(\mathbf{r}, \tau)] G(\mathbf{r}, \tau) + U^2 T_{pp}(\mathbf{r}, \tau) G(-\mathbf{r}, -\tau) \quad (3)$$

where  $\chi_{ph} = -G(\mathbf{r}, \tau) G(-\mathbf{r}, -\tau)$  and  $\chi_{pp} = G(\mathbf{r}, \tau) G(\mathbf{r}, \tau)$  are the particle-hole and particle-particle susceptibility bubbles. The density, spin, and particle fluctuation  $T$ -matrices are most simply written in momentum-frequency space,

$$T_{sf}(\mathbf{q}, \omega_m) = \frac{3}{2} \frac{U\chi_{ph}(\mathbf{q}, \omega_m)^2}{1 - U\chi_{ph}(\mathbf{q}, \omega_m)} \quad (4)$$

$$T_{\rho\rho}(\mathbf{q}, \omega_m) = -\frac{1}{2} \frac{U\chi_{ph}(\mathbf{q}, \omega_m)^2}{1 + U\chi_{ph}(\mathbf{q}, \omega_m)} \quad (5)$$

$$T_{pp}(\mathbf{q}, \omega_m) = \frac{U\chi_{pp}(\mathbf{q}, \omega_m)^2}{1 + U\chi_{pp}(\mathbf{q}, \omega_m)}. \quad (6)$$

The Green's function is obtained from Dyson's equation

$$G(\mathbf{k}, \varepsilon_n)^{-1} = G_o(\mathbf{k}, \varepsilon_n)^{-1} - \Sigma(\mathbf{k}, \varepsilon_n) \quad (7)$$

where  $G_o(\mathbf{k}, \varepsilon_n)$  is the non-interacting Green's function. The FEA self-energy (and therefore  $G$ ) are found from the self-consistent solution of Eqs. (3–7).

### §3 Numerical Methods and Analytic Considerations

We briefly describe our methods here; a more detailed account can be found elsewhere (Deisz, Hess and Serene, 1994). The self-consistent self-energy is obtained by the iterative solution of Eqs. (3–7). Efficient fast Fourier transforms are used to switch between  $(\mathbf{r}, \tau)$ -space and  $(\mathbf{k}, \varepsilon_n)$ -space. Since we use periodic boundary conditions on a periodic lattice, the use of discrete Fourier transform (DFT) methods introduces no fundamental difficulties in the transformation between  $\mathbf{k}$  and  $\mathbf{r}$  variables. On the other hand, a discrete sampling of the  $\tau$  variable generally introduces an artificial periodicity (with a period of the cutoff frequency) in the space of (discrete) Matsubara frequency. Nonetheless, all currently used high frequency cutoff schemes can be simulated using DFT's, with the possible cost of doubling the number of frequencies used (Serene and Hess, 1992). Building on the observation that comparatively little information is contained in the high frequency behavior of  $G$ , the  $T$ -matrices, the susceptibility bubbles, and  $\Sigma$ , we have devised a substantially more accurate method that preserves the formal internal self-consistency of the theory, improves the stability of the algorithm, and enables thermodynamic quantities to be calculated reliably. We decompose all quantities into the sum of a numerical term and an analytic term. The analytic terms are asymptotically exact at high frequency; they allow highly accurate calculations of contributions to low-frequency properties from convolution sums over high-frequency tails. These contributions, which propagate through any iterative solution of the nonlinear equations of the FEA, are lost in other implementations that introduce a high frequency cutoff. We find that accurate treatment of these contributions is absolutely essential for meaningful results from the FEA in the presence of large fluctuations. We perform calculations on  $128 \times 128$  lattices of  $\mathbf{k}$ -points with typically 512 Matsubara frequencies. A fine mesh is required to represent accurately important fine structure that evolves, especially in the spin-fluctuation propagator, with decreasing temperature. The resulting algorithm has yielded converged solutions at half-filling for a large range of  $U$  with continuous control of the temperature  $T$  down to  $T \sim 0.008t$  the lowest temperatures we have explored. Numerical analytic continuation of quantities calculated on the imaginary frequency axis to the real frequency axis is accomplished using Padé approximants (Vidberg and Serene, 1977).

The slowly decaying high frequency tails of the single-particle Green's function are a consequence of the discontinuity of  $G$  and its derivatives at  $\tau = 0$ . For example, the discontinuity  $G(0^+) - G(0^-) = -1$  (which follows from the canonical anticommutation relations for Fermions) results in the  $1/i\varepsilon_n$  behavior of  $G$  at high frequency. More

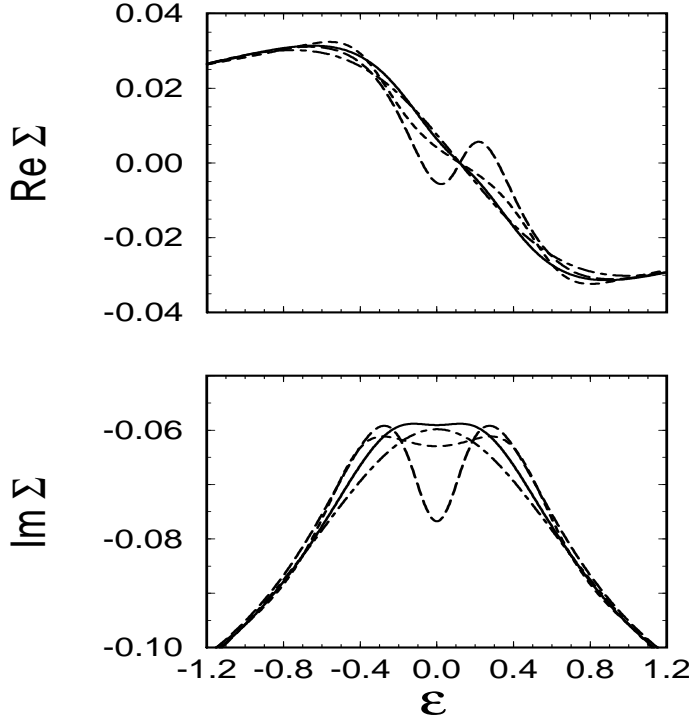


Figure 1: The evolution of a non-Fermi liquid self-energy with decreasing temperature. Shown are  $\Sigma(\mathbf{k}_F = (\pi/8, 7\pi/8), \varepsilon)$  for  $T = 0.06$  (long dash),  $0.07$  (dashed),  $0.09$  (solid) and  $0.12$  (dot-dash). Note that above  $\varepsilon \sim 1$ ,  $\text{Im } \Sigma(\mathbf{k}, \varepsilon)$  displays the linear behavior consistent with our earlier observations (Serene and Hess, 1992).

generally, discontinuities in  $G(\tau)$  and its derivatives can be related to weighted integrals of the spectral function,

$$\frac{\partial^n G(\mathbf{k}, \tau)}{\partial \tau^n} \Big|_{\tau=0^+} - \frac{\partial^n G(\mathbf{k}, \tau)}{\partial \tau^n} \Big|_{\tau=0^-} = (-1)^{(n+1)} \int_{-\infty}^{\infty} \varepsilon^n A(\mathbf{k}, \varepsilon) d\varepsilon. \quad (8)$$

The left hand side of this equation can be evaluated directly using the equations of motion for  $G$ , yielding exact sum rules for the single particle spectral function. From Dyson's equation for the exact  $G$  and the 'skeleton' diagram expansion for  $\Sigma$  one can show (Deisz, Serene and Hess, 1995) that for the Hubbard Hamiltonian: (1) the contribution from the self-energy to the  $n = 1$  sum rule comes entirely from the Hartree-Fock diagram with the exact  $G$ , and (2) the contribution from the self-energy to the  $n = 2$  sum rule comes entirely from the second-order 'skeleton' diagram evaluated with the exact  $G$ . When evaluated with the FEA Green's function, the first moment sum rule is satisfied but the second generally is not. It is important to note, however, that the violation of the sum rule is significantly greater for approximations that keep only particle-hole bubble contributions. From this point of view, the FEA is a better approximation than taking particle-hole bubble or particle-particle ladder 'skeleton' graphs alone.

#### §4 Neither Fermi-Liquid Nor Antiferromagnet

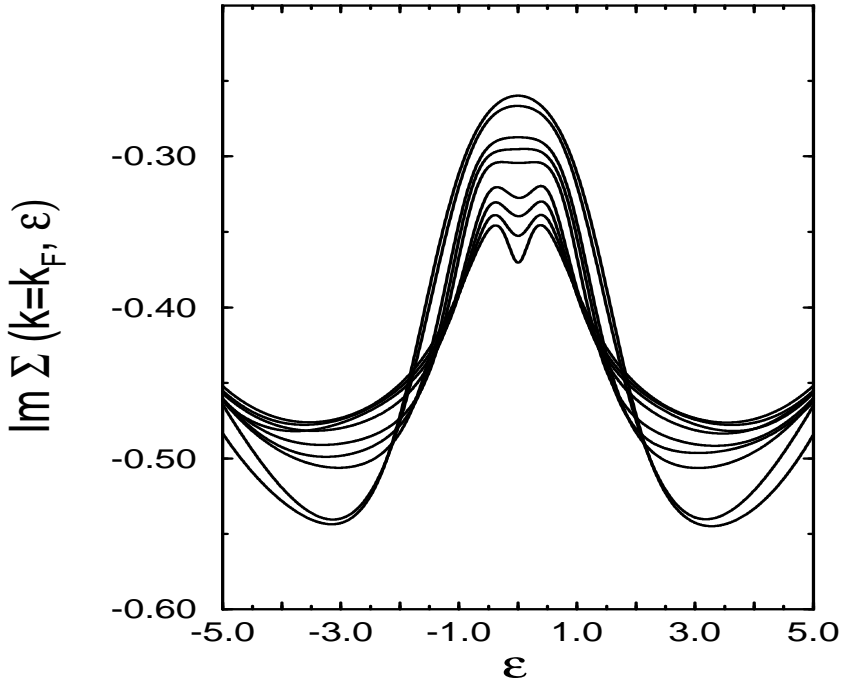


Figure 2:  $\text{Im } \Sigma(\mathbf{k}_F, \varepsilon)$  for  $U = 2.7$  and  $T = 0.10$  showing the smooth transformation from clear non-fermi liquid behavior at  $\mathbf{k} = (\pi, 0)$  on the Fermi surface (lowest curve at  $\varepsilon = 0$ ) to a Fermi-liquid like behavior at the point  $\mathbf{k} = (\pi/2, \pi/2)$  on the Fermi surface along the  $(1, 1)$  direction (highest curve at  $\varepsilon = 0$ ).

We have calculated self-consistent self-energies in the fluctuation exchange approximation for the 2D Hubbard model at half filling. In Fig. 1, we show the self-energy at low energy for a momentum on the Fermi surface near the  $X$  point and for various temperatures. For this modest  $U = 1.57$  (all energies are understood to be measured with respect to the hopping matrix element  $t$ ) we observe that at high temperature ( $T \gtrsim 0.12$ , approximately the mean field transition temperature) the energy dependence of  $\Sigma$  at low energy is roughly similar to that of Fermi liquid theory: the slope of  $\text{Re } \Sigma$  corresponds to a quasiparticle pole weight near unity, and  $\text{Im } \Sigma$  shows a roughly parabolic energy dependence. It is important to note, however, that  $\text{Im } \Sigma(\mathbf{k}_F, \varepsilon = 0)$  is significantly larger in magnitude compared with that calculated for an approximation containing only the second order diagram (Deisz *et al.*, 1995). This reflects enhanced quasiparticle-quasiparticle scattering by AFM spin fluctuations. As the temperature is lowered,  $\Sigma$  develops structure at  $\varepsilon = 0$  that is inconsistent with a Fermi liquid; the slope of  $\text{Re } \Sigma$  decreases rapidly and eventually changes sign, and  $\text{Im } \Sigma$  develops a local minimum. These anomalies occur at roughly half the mean field theory transition temperature to the antiferromagnetically ordered state in mean field theory. Moreover, the energy scale suggested by the local maxima in  $\text{Im } \Sigma$  at  $\varepsilon \sim 0.28$  is very nearly the size of the zero temperature gap  $\Delta$  in mean field theory obtained by the  $\mathbf{k}$ -sum over the

magnetic Brillouin zone,

$$U^{-1} = \frac{1}{N} \sum_k \frac{1}{\sqrt{\epsilon_k^2 + \Delta^2}}. \quad (9)$$

We have found this near agreement to hold for several values of  $U$  less than half of the bandwidth. In a separate work, (Deisz, *et. al.*, 1995) we have shown from calculated single-particle spectral functions that the evolution of the anomaly is accompanied by a dramatic suppression of spectral weight at the Fermi surface. The loss in spectral weight at the Fermi surface leads to a formation of a weak pseudogap in the density of states at  $\varepsilon = 0$ . As shown in Fig. 2, the evolution of the anomaly is anisotropic; it starts at the  $X$  point and spreads across the Fermi surface with decreasing temperature.

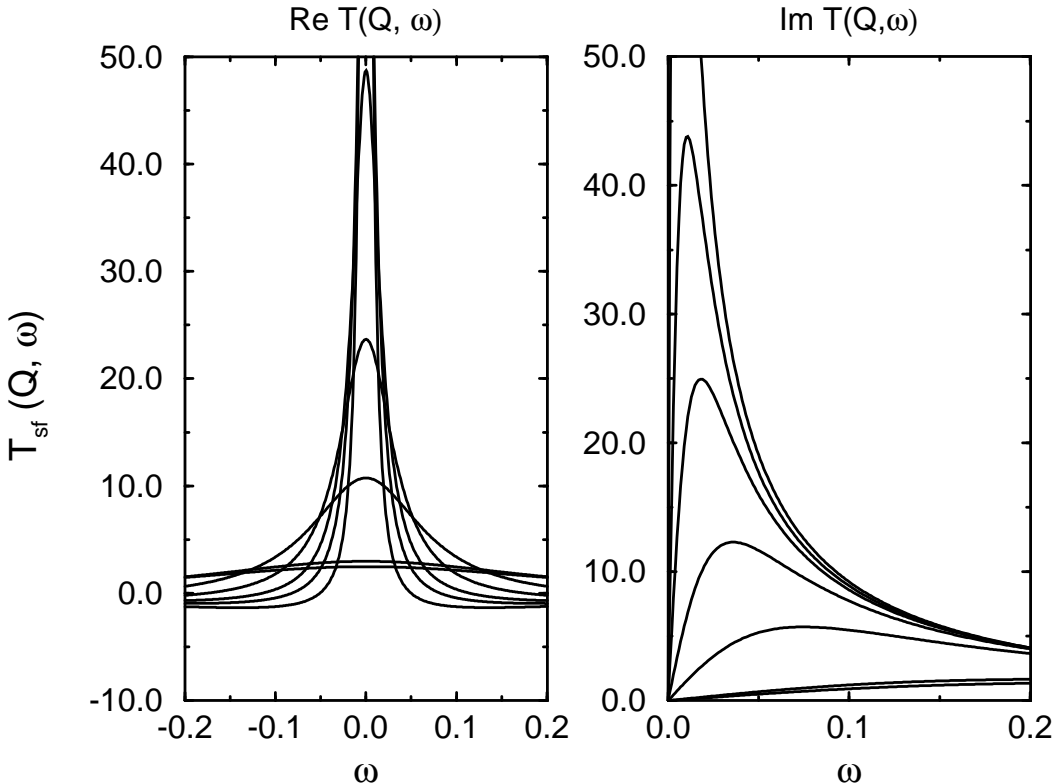


Figure 3: The monotonic evolution with decreasing temperature of sharply peaked structure in the spin-fluctuation  $T$ -matrix  $T_{sf}$  on the real energy axis at  $\mathbf{Q} = (\pi, \pi)$ . Shown are  $\text{Re } T_{sf}(\mathbf{Q}, \omega)$  and  $\text{Im } T_{sf}(\mathbf{Q}, \omega)$  for  $T = 0.20, 0.18, 0.10, 0.08, 0.07, 0.065, 0.06$

The appearance of the non-Fermi liquid state is presaged by the evolution and rapid growth with decreasing temperature of structure in the spin-fluctuation  $T$ -matrix that is sharply peaked in momentum at  $\mathbf{Q} = (\pi, \pi)$  and in Matsubara frequency about  $\omega_m = 0$ . The analytic continuation of  $T_{sf}(Q, \omega_m)$  to the real frequency axis is shown in Fig. 3. The rapid increase in  $T_{sf}(Q, \omega = 0)$  is shown in detail together with the temperature dependence of the width of the peak in frequency  $\Delta_\omega T_{sf}$  and momentum  $\Delta_\mathbf{q} T_{sf}$  (for high temperature, the latter quantity is anisotropic and the width is for the  $\hat{k}_x$  direction). Also plotted in the lower panel of Fig. 4 is  $1/T_{sf}(Q, \omega = 0)$ . Below  $T \sim 0.07$ ,  $\Delta_\omega T_{sf}$

and  $1/T_{sf}(Q, \omega = 0)$  track each other closely suggesting the existence of a characteristic temperature  $T^*$  below which the behavior of  $T_{sf}(Q, \omega)$  can be characterized by a simple diffusive pole at a (temperature dependent) characteristic energy  $\omega^*$ . It is interesting to note that  $\omega^*$  decreases rapidly with decreasing temperature below  $T^*$  and the admittedly small amount of data available below  $T^*$  can be approximated well by the functional form  $T_{sf}(Q, 0) = B \exp(A/T)$ . We note that the structure of  $T_{sf}(\mathbf{q} \sim \mathbf{Q}, \omega)$  below  $T^*$  is similar to that of the spin-spin correlation function proposed by Millis, Monein and Pines, 1989. In contrast,  $T_{sf}(\mathbf{q}, \omega)$  presented here is the result of a fully self-consistent calculation and  $T_{sf}(\mathbf{q}, \omega)$  cannot be observed directly in an experiment; a fully self-consistent calculation of the dynamical spin-spin response function is necessary to determine how  $\omega^*$  is expressed in measurable magnetic properties.

We emphasize that the rapid rise in  $T_{sf}(Q, 0)$  with decreasing temperature need not be reflected in any physically measurable response function and does not necessarily signal a phase transition. The fully self-consistent staggered spin susceptibility as a function of temperature is presented in Fig. 5. The staggered spin susceptibility was calculated from a trace of the self-consistent Green's functions in the presence of an applied staggered field. The absence in  $\chi_{AFM}$  of any reflection of the rapid rise in  $T_{sf}(Q, 0)$ , dramatically contrary to expectations from an RPA calculation of the response, shows the importance of vertex corrections in the FEA response functions near an instability.

## §5 Beyond FEA: Calculations in Parquet Approximations

De Dominicis (De Dominicis, 1963) reformulated the propagator renormalized perturbation theory of Luttinger and Ward to eliminate not only the single-particle potentials in favor of single-particle Green's function but also to eliminate the two-body potential in favor of the two-particle propagator  $G_2$  (or equivalently the two-particle vertex function). In this theory, the entropy  $S$  plays a role analogous to that of the grand potential in the theory of Luttinger and Ward; the entropy may be viewed as a functional of  $G$ ,  $\Sigma$ ,  $G_2$  and the two-particle vertex function  $\Gamma$ . The stationarity conditions for  $S$  with respect to variations of  $G$ ,  $\Sigma$ ,  $G_2$  and  $\Gamma$  constitute a closed set of equations that must be solved self-consistently. Here we present the equations for the two-particle self-consistent perturbation theory schematically and refer the interested reader to the original works for the full formulation. These are the: Dyson's equation for the single particle propagator in Eq. (7); a relation between the self-energy, the bare interaction  $U$ , and the renormalized two-particle vertex function

$$\Sigma = UGG\Gamma, \quad (10)$$

which includes implicit double integrals over momenta and double sums over frequency; the decomposition of the vertex function in terms of a fully two-particle irreducible vertex  $V$  and  $T$ -matrices in particle-hole, crossed particle-hole, and particle-particle channels,

$$\Gamma = V + T_{ph} + \tilde{T}_{ph} + T_{pp}; \quad (11)$$

and a set of Bethe-Salpeter equations relating a  $T$ -matrix in the  $i$ -th channel to a vertex function  $I_i$  that is two-particle irreducible in that channel

$$T_i = I_i G G I_i + I_i G G T_i. \quad (12)$$

This set of equations is closed by expressions relating each vertex  $I_i$  to the  $T$ -matrices and  $V$ . The resulting theory is self-consistent at the level of the single- and two-particle propagators.

We have solved these equations on the CM-5, using a parallel algorithm we describe elsewhere (Hess and Serene, 1995), for small Hubbard chains. We employ two additional approximations in our parquet approximation calculations that are outside the framework of the exact theory: the fully two-particle irreducible vertex  $V$  is taken to be the bare Hubbard interaction, and a high frequency cutoff is imposed with periodic boundary conditions in discrete frequency space (see Deisz, *et al.*, 1994). Both of these approximations may be relaxed (Hess and Serene, 1995).

In Fig. 6, we show the single-particle propagator  $G(\mathbf{k}, \tau)$  calculated in the parquet approximation described above, together with  $G(\mathbf{k}, \tau)$  from various single-particle self-consistent approximations including the FEA, the shielded potential approximation (includes only the particle-hole bubble diagrams together with the second order diagram), the T-approximation (includes only particle-particle ladder diagrams together with the second order diagram), and an approximation including only the second-order diagram. The self-consistent calculations were all performed using the same high frequency cutoff scheme. For comparison we show  $G(\mathbf{k}, \tau)$  obtained from quantum Monte Carlo (Assaad, 1995). Because of the increased importance of fluctuations in 1D, we expect that the FEA, shielded potential approximation and T-approximations to be poor. Of all the diagrammatic approaches shown here, the parquet approximation is closest to the quantum Monte Carlo result for a  $U$  equal to one quarter of the bare bandwidth. In agreement with our sum-rule argument in §3, the FEA provides a better approximation than shielded potential approximation. The approximation containing only the second-order ‘skeleton’ diagram is in better agreement with QMC than any of the other single-particle self-consistent theories, at least for this relatively small  $U$ . This may in part reflect the better agreement with the second moment sum-rule on the single-particle spectral function.

## §6 Conclusions

We have shown that the coupling of spin-fluctuations to quasiparticles, as both evolve with decreasing temperature, leads to the formation of a non-Fermi liquid state in the 2D Hubbard model at half-filling in the fluctuation exchange approximation. The non-Fermi liquid state shows a positive slope in the real part of sigma and a local minimum in the imaginary part at zero energy. The energy scale over which these anomalies extend is roughly the size of the zero temperature gap in mean field theory. We have shown that this behavior is preceded by the evolution of a sharp peak the spin-fluctuation  $T$ -matrix at  $\mathbf{Q} = (\pi, \pi)$  and that the evolution of this structure continues with decreasing temperature. An analysis of the  $T$ -matrix suggests the existence of two temperature regimes separated by a characteristic temperature  $T^*$ . For temperatures above  $T^*$ , the self-energy does not show the anomaly; for temperatures below  $T^*$ , the anomaly in the self-energy is present and the sharp structure in the  $T$ -matrix can be described by a single temperature dependent energy scale  $\omega^*$  which decreases rapidly with decreasing temperature. While the FEA may provide a useful model for coupled quasiparticles and spin-fluctuations that self-consistently includes the effects of evolving low-energy anomalies, it is both desirable and possible to go beyond the FEA. We presented calculations that are self-consistent at the levels of both the single- and two-particle propagators for

the Hubbard model in 1D. Two approximations were employed: replacing the fully two-particle irreducible interaction by the bare interaction, and imposing a high frequency cutoff. Our results for the single particle propagator suggest the importance of vertex corrections in calculating the self-energy and compare favorably with quantum Monte Carlo calculations. In future work we will explore the sensitivity of our results to the structure of the fully two-particle irreducible interaction and discuss the structure of the vertex function.

## Acknowledgements

We thank F. Assaad for supplying quantum Monte Carlo results for the 1D Hubbard model. It is a pleasure to acknowledge useful discussions with A. Kampf, A. Millis, and D. Pines. One of us (DH) would like to thank Lisa Noordergraaf, Bob Weisbeck and Mike Young at the NRL CMF for useful discussions. This work was supported in part by a grant of computer time from the Office of Naval Research and the DoD HPC Shared Resource Centers: Naval Research Laboratory Connection Machine facility CM-5; Army High Performance Computing Research Center under the auspices of Army Research Office contract number DAAL03-89-C-0038 with the University of Minnesota.

## References

Anderson, P.W., 1987, *Science* **235**, 1196.

Anderson, P.W., 1990, *Phys. Rev. Lett.* **64**, 1839.

Assaad, F., 1995, private communication.

Baym, G, and Pethick, C.J., 1991, *Landau Fermi-Liquid Theory*, (Wiley, New York).

Berk, N., and Schrieffer, J.R., 1966, *Phys. Rev. Lett.* **17**, 433.

De Dominicis, C. N., 1963, *J. Math. Phys.* **4**, 255.

Dagotto, E., 1994, *Rev. Mod. Phys.* **66**, 763.

Deisz, J.J., Hess, D.W., and Serene, J.W., 1994, *Recent Progress in Many-Body Theories*, vol. 4, edited by E. Schachinger, *et al.*, Plenum, New York.

Deisz, J.J., Hess, D.W., and Serene, J.W., 1995, *Bull. Am. Phys. Soc.* **40**, 504; Deisz, J.J., Hess, D.W., and Serene, J.W., 1995, preprint.

Deisz, J.J., Serene, J.W., and Hess, D.W., 1995, in preparation.

Doniach, S. and Engelsberg, S., 1966, *Phys. Rev. Lett.* **17**, 750.

Hess, D.W. and Serene, J.W., in preparation.

Hirsch, J.E., and Tang, S., 1989, *Phys. Rev. Lett.* **62**, 591.

Kampf, A.P., 1994, *Phys. Rep.* **249**, 219.

Luttinger, J.M., and Ward, J.C., 1960, *Phys. Rev.* **118**, 1417.

Millis, A., Monien, H., and Pines, D., 1990, *Phys. Rev. B* **42**, 167.

Pines, D., 1990, *Physica B* **163**, 78.

Serene, J.W., and Hess, D.W., 1992, *Recent Progress in Many-Body Theories*, vol. 3, edited by T.L. Ainsworth *et al.*, Plenum, New York.

White, S.R., Scalapino, D.J., Sugar, R.L., Loh, E.Y., Gubernatis, S.E., and Scalettar, R.T., 1989, *Phys. Rev. B* **40**, 506.

Vidberg, H.J., Serene, J.W., 1977, *J. Low Temp. Phys.*, **19**, 179.

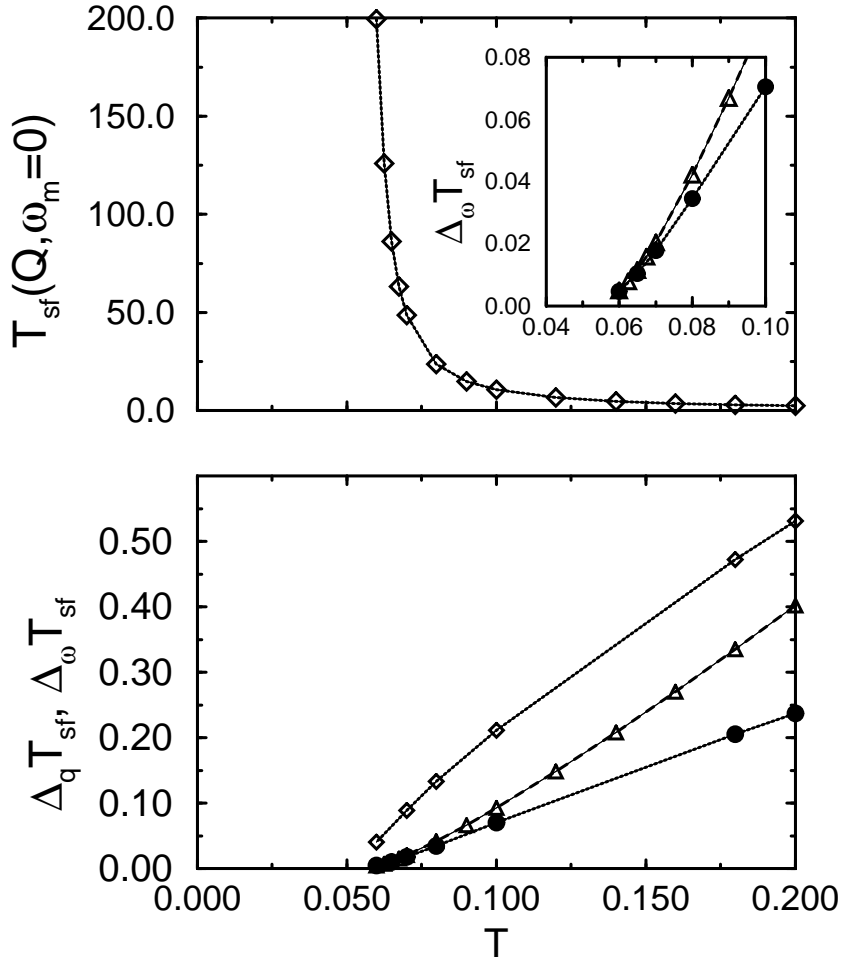


Figure 4: The evolution of the sharply peaked structure of the spin fluctuation  $T$ -matrix  $T_{sf}$  with decreasing temperature: (top panel) The maximum of  $T_{sf}$  at  $\mathbf{Q}$  and  $\omega = 0$  as a function of  $T$ ; (bottom panel) the temperature dependence of the HWHM of the sharp peak in  $T_{sf}$  in momentum  $\Delta_q T_{sf}$  ( $\diamond$ ), the HWHM of  $T_{sf}(\mathbf{Q}, \omega)$   $\Delta_\omega T_{sf}$  ( $\bullet$ ), and  $1/T_{sf}(\mathbf{Q}, 0)$  ( $\triangle$ ). The inset shows the merging of  $\Delta_\omega T_{sf}$  with  $1/T_{sf}(\mathbf{Q}, 0)$  below the temperature  $T^*$  (see text).

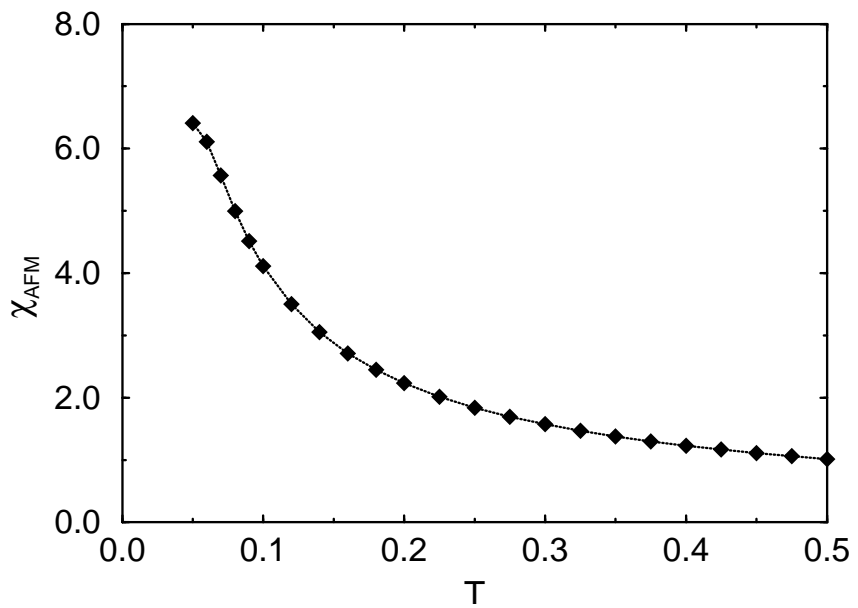


Figure 5: The fully self-consistent spin response for  $\mathbf{q} = \mathbf{Q} = (\pi, \pi)$ . Note that  $\chi_{AFM}(T)$  does not display the rapid increase with decreasing  $T$  that is observed in  $T_{sf}(\mathbf{Q}, 0)$ .

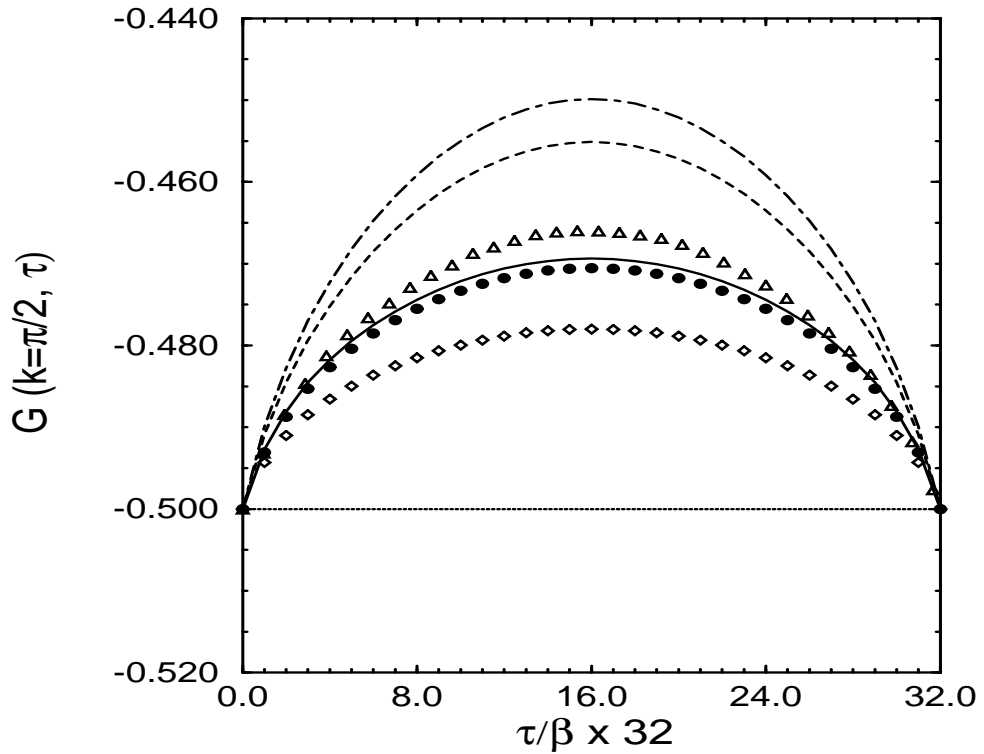


Figure 6: The single-particle Green's function  $G(\mathbf{k} = \pi/2, \tau)$  for an eight-site half-filled Hubbard chain for  $U = t$  and  $T = 0.20$  calculated in the parquet approximation (solid) compared with the bare propagator (dotted), quantum Monte Carlo ( $\triangle$ ), and the single-particle self-consistent perturbation theories: the second order diagram alone ( $\bullet$ ), the  $T$  approximation ( $\diamond$ ), the shielded potential approximation (dot-dash), and the fluctuation exchange approximation (dashed). Note that of the self-consistent perturbation theory calculations, the parquet approximation agrees most closely with the quantum Monte Carlo result.